JACS
JOURNAL OF THE AMERICAN CHEMICAL SOCIETY

ARTICLE

pubs.acs.org/JACS

Twisted π-System Chromophores for All-Optical Switching

Guang S. He,[†] Jing Zhu,[†] Alexander Baev,[†] Marek Samoć,[*,†,§] David L. Frattarelli,[‡] Naoki Watanabe,[‡] Antonio Facchetti,[*,‡] Hans Ågren,[*,#] Tobin J. Marks,[*,‡] and Paras N. Prasad[*,†]

[†]The Institute for Lasers, Photonics and Biophotonics, State University of New York at Buffalo, Buffalo, New York 14260, United States
[‡]Department of Chemistry and the Materials Research Center, Northwestern University, Evanston, Illinois 60208, United States
[§]Institute of Physical and Theoretical Chemistry, Wroclaw University of Technology, 50370 Wroclaw, Poland
[#]Theoretical Chemistry, Royal Institute of Technology, SE-100 44 Stockholm, Sweden

Supporting Information

ABSTRACT: Molecular chromophores with twisted π-electron systems have been shown to possess unprecedented values of the quadratic hyperpolarizability, β, with very large real parts and much smaller imaginary parts. We report here an experimental and theoretical study which shows that these twisted chromophores also possess very large values of the real part of the cubic hyperpolarizability, γ, which is responsible for nonlinear refraction. Thus, for the two-ring twisted chromophore **TMC-2** at 775 nm, relatively close to one-photon resonance, n_2 extrapolated to neat substance is large and *positive* (1.87×10^{-13} cm^2/W), leading to self-focusing. Furthermore, the third-order response includes a remarkably low two-photon absorption coefficient, which means minimal nonlinear optical losses: the T factor, $\alpha_2\lambda/n_2$, is 0.308. These characteristics are attributed to closely spaced singlet biradical and zwitterionic states and offer promise for applications in all-optical switching.

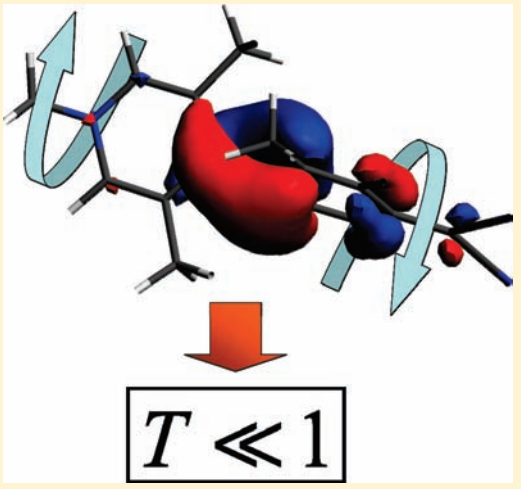

INTRODUCTION

The development of high-performance molecule-based nonlinear optical (NLO) materials has been the focus of intense current research. Such materials are of great scientific and technological interest not only for applications as diverse as optical telecommunications, signal processing, data storage, image reconstruction, logic technologies, and optical computing, but also for the fundamental understanding of how soft matter interacts with light.[1−3] The essential requirement for large bulk NLO response is that the active component chromophores have a large microscopic molecular second-order (quadratic hyperpolarizability, β) or third-order (cubic hyperpolarizability, γ) tensor. In the simplest molecular description, both β and γ can be described by conventional two-level and three-level models, respectively, and most approaches to maximizing β and γ have been intuited from these models:[4]

$$\beta \propto (\mu_{ee} - \mu_{gg}) \frac{\mu_{eg}^2}{E_{eg}^2}$$
$$\gamma \propto -\frac{\mu_{eg}^4}{E_{eg}^3} + \frac{\mu_{e'e}^2 \mu_{eg}^2}{E_{eg}^2 E_{e'g}} + \frac{\mu_{eg}^2 (\mu_{ee} - \mu_{gg})}{E_{eg}^3} \quad (1)$$

where μ_{ij} and $\mu_{\kappa\kappa}$ are transition and permanent dipole moments, respectively, and E_{ij} is the transition energy. Successful approaches to enhancing β and γ have included tuning the molecular bond length alternation characteristics.[5] Another strategy[6] correlates β with π-conjugation electron density and involves introducing electron-rich and electron-deficient heterocyclic bridges, which act as auxiliary donors and acceptors, into the molecular skeleton. Directed by these strategies, large β values have been achieved in planar linear polyenes and/or by incorporating multiple heterocycle-containing bridges, with $\mu\beta$ (μ = dipole moment) values as high as $30\,000 \times 10^{-48}$ esu reported.[5,6] Importantly, these conventional β and γ enhancement strategies have focused on extended planar linear π-conjugation, where the π-system is charge-neutral, and have significant known NLO response and stability limitations.[7] Other β enhancement strategies include implementing multidimensional charge-transfer chromophores,[8] which exhibit enhanced optical transparency and thermal stability; however, significant β enhancement has not been observed to date. Interestingly, Kuzyk has argued that the β and γ responses of all known organic chromophores fall far short of the fundamental limits.[9] This raises the intriguing question of whether there exist alternative strategies for producing very large γ chromophores.

Received: December 15, 2010
Published: April 07, 2011

   dx.doi.org/10.1021/ja1113112 | J. Am. Chem. Soc. 2011, 133, 6675–6680

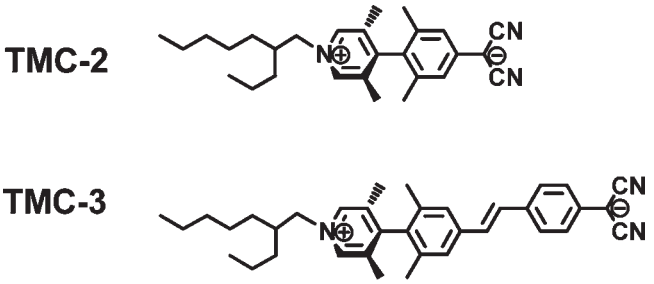

Figure 1. Chemical structure of twisted chromophores **TMC-2** and **TMC-3**.

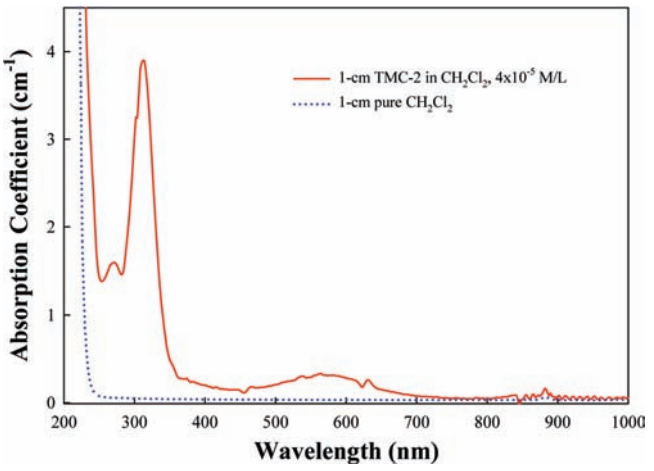

Figure 2. Optical absorption spectra of a **TMC-2** solution in CH_2Cl_2 and of pure CH_2Cl_2.

Recent research has demonstrated a new NLO chromophore design paradigm: twisted π-electron system chromophores (Figure 1), which were first discovered theoretically,[6a,10] then synthesized and characterized by a variety of experimental and theoretical techniques.[11,12] They achieve β values, measured by concentration-dependent electric field-induced second harmonic generation techniques, as high as 10−15 times larger than those of any previously reported molecular chromophore of comparable size ($\mu\beta = -488\,000 \times 10^{-48}$ esu at 1907 nm for **TMC-3**), and poled guest−host polymers exhibit electro-optic coefficients as high as 330 pm/V at 1310 nm. Without long extents of conjugated double bonds, these chromophores exhibit excellent thermal and oxidative stabilities.[11] Furthermore, electronic structure computation pinpoints the importance of closely spaced singlet biradical and zwitterionic states, which greatly reduce the denominator energy terms in eq 1, and thus substantially enhance β.[12] Twisted chromophore nonlinear response can be further tuned by both structure modification and solvation effects. Note that analogous planar chromophores possess far smaller β values, confirming the importance of the twist enhancement mechanism.[11a] Importantly, these new chromophore design paradigms are significantly different from previous NLO strategies. The intriguing question then arises as to whether this enhancement mechanism might be applicable to γ as well, because the same terms contribute to the energy denominator, as shown in eq 1. Moreover, in contrast to expectations for β and the macroscopic quadratic susceptibility $\chi^{(2)}$, acentric structures

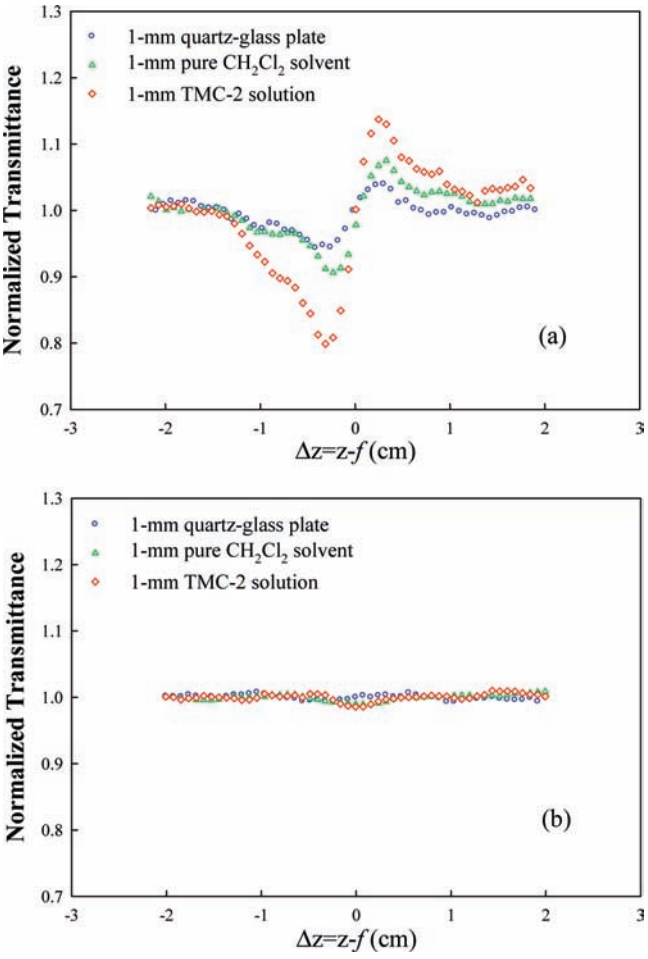

Figure 3. Z-scan results for 1-mm-thick chromophore solution, quartz-glass, and pure solvent samples measured at ~775 nm wavelength: (a) closed aperture with an $L = 40$ cm distance from the sample and an input pulse energy of 0.73 μJ; (b) open aperture with an $L = 7$ cm distance from the sample and an input pulse energy of 1.2 μJ.

and poling are not required for the existence of the macroscopic cubic susceptibility $\chi^{(3)}$. In this contribution, we report a combined experimental and theoretical study of chromophore **TMC-2** ($\mu\beta = -24\,000 \times 10^{-48}$ esu) which shows that these twisted chromophores also possess very large values of the real part of the cubic hyperpolarizability γ, which is responsible for nonlinear refraction. The twisted chromophore third-order response also includes a rather low imaginary component, which means minimal nonlinear optical losses. It will be seen that these characteristics are attributable to closely spaced singlet biradical and zwitterionic states and offer promise for applications in all-optical switching. Indeed, as was mentioned before, biradical states are close-lying in energy and have large interstate transition moments, two features that make up for large sum-over-states NLO coefficients (eq 1). In fact, this can be understood from a three-states model: the biradical ground state S0 has a HOMO−LUMO mixing, the first excited singlet state S1 is of HOMO→LUMO character, and the second excited singlet state S2 has a HOMO+LUMO mixing, implying strong S0−S1 and S1−S2 transition dipole moments. For further reading on NLO response of biradicals, we refer to work by Nakano and co-workers.[13]

dx.doi.org/10.1021/ja1113112 |J. Am. Chem. Soc. 2011, 133, 6675–6680

RESULTS AND DISCUSSION

Measurements. Figure 2 shows the linear absorption spectra of the **TMC-2** chromophore[11a,b] as a solution in CH_2Cl_2 and of the pure solvent. The optical path length for both samples is 1.0 cm. From this figure it can be seen that the solute has a strong UV absorption band peaking at ~ 310 nm and a relatively weak but broader absorption band in the 570 nm range. For such a solution sample, the cubic NLO response is due to the third-order nonlinear susceptibility, which can be expressed as in eq 2,

$$\chi^{(3)} = L^4(N_{solv}\gamma_{solv} + N_{solute}\gamma_{solute}) \cong (1-x)\chi^{(3)}_{solv} + x\chi^{(3)}_{solute} \quad (2)$$

where x is the molar fraction of the solute, the first term on the right-hand side is the contribution from the solvent, and the second term is the contribution from the solute. In the present case, the solvent has no nonlinear absorption in the spectral range of interest, and therefore $\chi^{(3)}_{solv}$ can be recognized as a real quantity; however, the chromophore exhibits certain characteristic nonlinear absorption features, and $\chi^{(3)}_{solute}$ must be treated as a complex quantity. Furthermore, $\chi^{(3)}_{solute}$ can be straightforwardly determined from separate measurements of $\chi^{(3)}$ and $\chi^{(3)}_{solv}$. Knowing $\chi^{(3)}_{solute}$ and the solute molar concentration, the real and imaginary parts of the nonlinear polarizability, γ, can be determined for the chromophore molecule and the macroscopic nonlinear parameters n_2 and α_2 assessed for a material containing a given chromophore concentration, e.g., the neat solid chromophore.

It is known that the real part of $\chi^{(3)}$ leads to an induced refractive index change which is described by $\Delta n = n_2 I$, while the imaginary part is responsible for the nonlinear (two-photon) absorption characterized by the value of α_2. For a given nonlinear optical medium, there are several different approaches to measuring these two parts separately. Z-scan is one of the commonly utilized methods to perform $\chi^{(3)}$ measurements. The advantage of this method is that both the real and imaginary parts of $\chi^{(3)}$ can be determined simultaneously or consecutively, using the so-called closed-aperture and open-aperture conditions, respectively.[14] In the present experiments, a 0.01 M solution of **TMC-2** in CH_2Cl_2 was contained in a 1.0 mm path-length quartz cell for Z-scan measurements, performed separately at 775 and 1172 nm wavelengths (see Supporting Information for more details). Under the same experimental conditions with an open or closed aperture, a solution sample was measured, then a solvent sample, and then a quartz-glass sample with 1.0 mm thickness. Utilizing the quartz-glass as a standard, with its known $\chi^{(3)}$ values,[15] one can determine the corresponding values of the solute itself on the basis of the obtained Z-scan curves of these three samples. Figure 3 shows the Z-scan results for twisted chromophore **TMC-2** measured with 775 nm laser pulses, while Figure 4 shows the results measured with 1172 nm laser pulses. Based on the Z-scan measurement results and the data processing procedure described in ref 15, the third-order nonlinearity parameters for the twisted π-system chromophore can be extracted and are summarized in Table 1. From these data, it

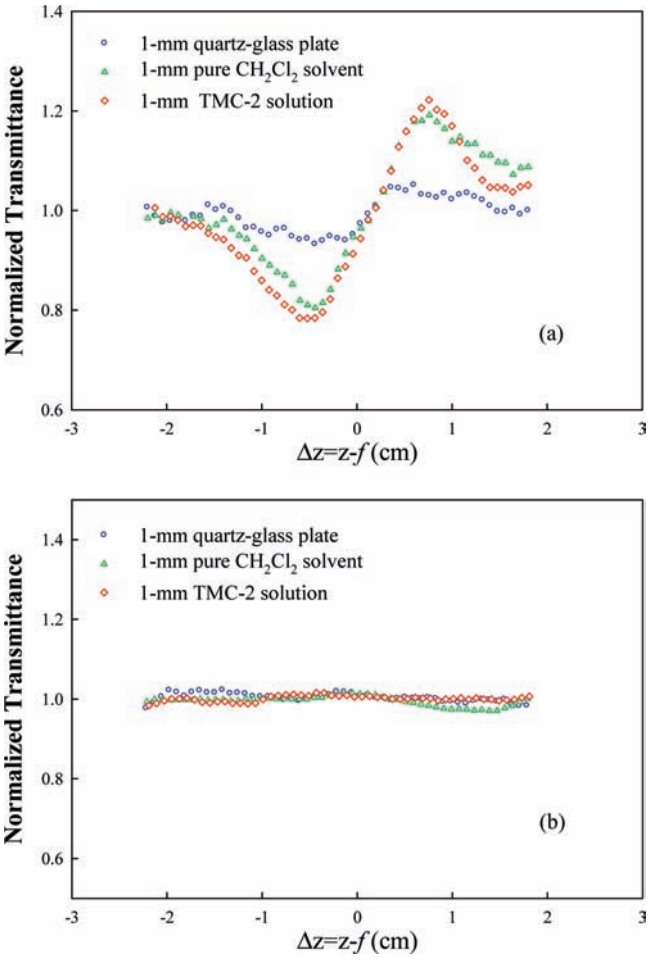

Figure 4. Z-scan results for 1-mm-thick solution, quartz-glass, and pure solvent samples measured at ~1172 nm wavelength: (a) closed aperture with an L = 40 cm distance from the sample and an input pulse energy of 2.4 μJ; (b) open aperture with an L = 5 cm distance from the sample and an input pulse energy of 2.4 μJ.

Table 1. Open- and Closed-Aperture Z-Scan Measurement Data for the Third-Order Nonlinearity Parameters of Twisted π-System Chromophore TMC-2

wavelength	775 nm	1170 nm
n_2 extrapolated to solute	1.87×10^{-13} cm^2/W	6.6×10^{-14} cm^2/W
Re($\chi^{(3)}$) extrapolated to solute	9.75×10^{-12} esu	3.4×10^{-12} esu
Re(γ)	1.4×10^{-33} esu	5.0×10^{-34} esu
2PA coefficient α_2 extrapolated to solute	7.42×10^{-10} cm/W	$<1.8 \times 10^{-10}$ cm/W
two-photon cross section σ_2	8.87 GM	1.5 GM
Im($\chi^{(3)}$) extrapolated to solute	2.38×10^{-13} esu	$<9 \times 10^{-14}$ esu
Im(γ)	3.43×10^{-35} esu	$<1.3 \times 10^{-35}$ esu
T factor	0.308	<0.32

can be seen that **TMC-2**, a relatively low response twisted chromophore having $\mu\beta = -24\,000 \times 10^{-48}$ esu, exhibits a large nonlinear refractive index coefficient, n_2, that is (in absolute terms) on the same order of magnitude as those for many extended π-conjugated polymers (e.g., poly-*p*-phenylenevinylenes) at the same wavelengths.[16] However, twisted chromophore **TMC-2** offers the following attractions: (1) At 775 nm, relatively close to the one-photon resonance, Re(γ) and thus n_2 are *positive* (leading to self-focusing), in contrast to most known third-order chromophores, such as **Se-7C** recently reported by Hales et al.[17] (Figure 5), and other polymethines for which n_2 is *negative* above half the band gap. (2) The two-photon absorption coefficient of **TMC-2** is remarkably low, yielding a *T* factor ($T \equiv \alpha_2\lambda/n_2 \ll 1$) suitable for all-optical switching devices.[18] (3) The twisted chromophore is also dimensionally relatively small, so much room remains for properties enhancement through tuning and extending the π-electron system.

Computational Analysis. To compute the first and second degenerate polarizabilities of twisted chromophore **TMC-2**, and thus better understand the response mechanism, TDDFT response theory was applied in two quantum chemistry packages, the Amsterdam Density Functional package[19] and Dalton.[20] The geometry (Figure 6), with the most important parameter being the inter-ring torsion angle, θ, was optimized at the semiempirical PM3 level. Agreement with the experiments[11] was satisfactory. Reference 11b quotes the torsion angle to be 89.6° according to an X-ray diffraction study. The angle derived from the solution-phase nuclear Overhauser effect data is 88 ± 10°.[11b] The computed torsion angle for the original **TMC-2** is 84.4°, in excellent agreement. This computation assumes a gas-phase environment (isolated molecule) and does not account for solvation effects, resulting in a slight discrepancy between the numbers.

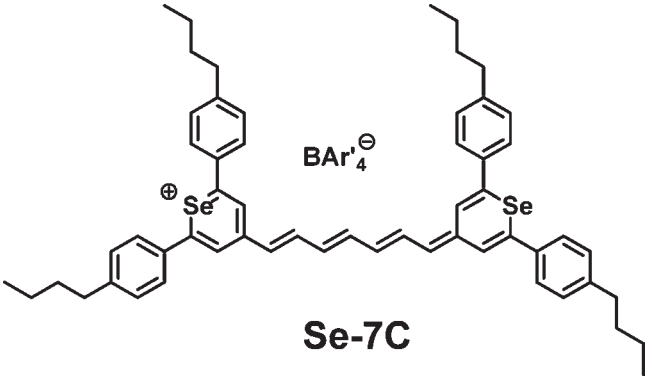

Figure 5. Chemical structure of the **Se-7C** chromophore.[17]

All computations of γ were performed for the degenerate $\gamma(\omega;\omega,-\omega,\omega)$ at the wavelengths corresponding to the telecommunication window. Once again, interest in the degenerate second hyperpolarizability, first and foremost, stems from the particular application of interest—all-optical switching—where the real part of the nonresonant degenerate third-order susceptibility determines the intensity-dependent refractive index of the medium described by n_2. While the functional used in these initial calculations (see Supporting Information) may somewhat overestimate γ and underestimate the lowest excitation energies, the results of the *ab initio* computations are in reasonable agreement with experiment, especially at the longer wavelength away from the one-photon resonance (see Table 2). These preliminary results give us confidence that twisted π-system chromophores have the potential for achieving breakthrough γ values, as already achieved for β.[11]

To analyze the mechanism of twist chromophore third-order susceptibility enhancement, an analysis of the computed $\gamma(\omega;\omega,-\omega,\omega)$ in terms of localized molecular orbitals was performed.[21] So-called natural localized molecular orbitals (NLMOs) were employed,[22] and the NLMO analysis reveals that a trio of π orbitals can be associated almost completely with the overall enhancement in γ. This trio of orbitals is shown in Figure 7. Their contribution to the averaged γ mostly stems from the xxxx component of the tensor, i.e., along the axis, connecting donor and acceptor groups. Notably, the contribution from the bridge orbital to this tensor component is virtually absent in the response of "untwisted" planar π-conjugated molecules. For example, consistent with the push−pull NLO mechanism, the π orbitals of the aryl bridge were previously shown to make an insignificant contribution to the magnitude of γ in *p*-nitroaniline molecules,[21] the more dominant contributors to the nonlinear

Table 2. Dispersion of the Averaged Degenerate First and Second Hyperpolarizabilities of Twisted Chromophore TMC-2 Computed with the PBE Functional

wavelength (nm)	β_{av} (10^3 au)	γ_{av} (10^5 au)	γ_{av} (esu)
775	384.79	~10^4	~5.04×10^{-31}
800	1787.38	>10^4	>5.04×10^{-31}
1000	22.42	940.62	4.74×10^{-32}
1300	17.62	13.31	6.70×10^{-34}
1550	15.38	2.92	1.47×10^{-34}
1700	14.59	1.23	6.19×10^{-35}
2000	13.61	−0.13	-6.55×10^{-36}
4000	11.96	−0.09	-4.53×10^{-36}
8000	11.59	0.04	2.01×10^{-36}
Inf	11.48	0.08	4.03×10^{-36}

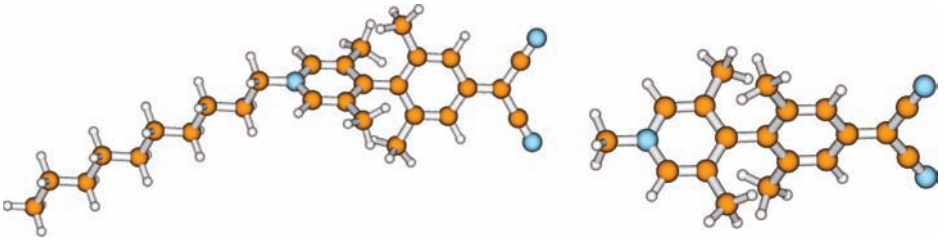

Figure 6. Computed molecular structures for twisted chromophore **TMC-2**: (left) with long side-chain for solubility, torsion angle 84.4°; (right) shortened structure for detailed computations, torsion angle 63.9°.

dx.doi.org/10.1021/ja1113112 |*J. Am. Chem. Soc.* 2011, 133, 6675–6680

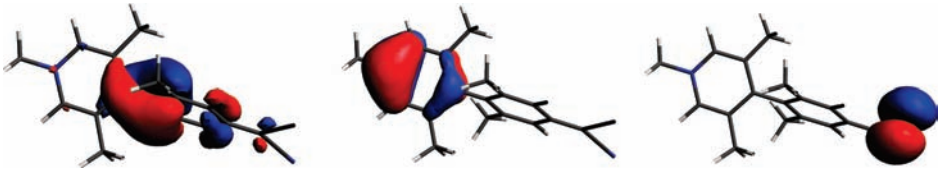

Figure 7. Field-free **TMC-2** NLMOs whose contributions account for the enhancement of the averaged value of the twisted chromophore second hyperpolarizability. From left to right: bridge NLMO, acceptor NLMO, and donor NLMO.

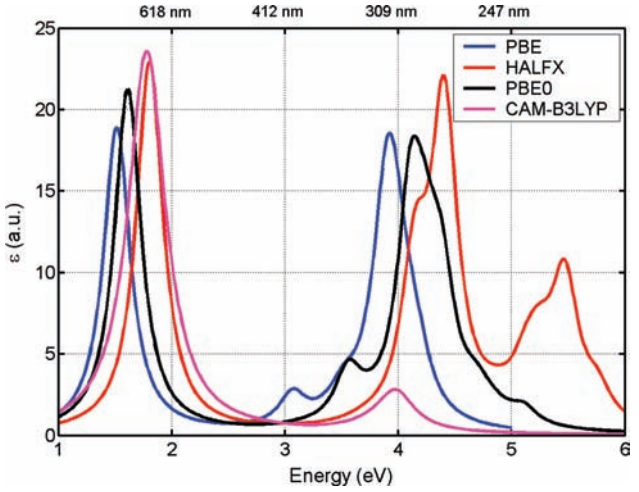

Figure 8. **TMC-2** absorption spectra calculated with the four different functionals described in the text.

response being the nitrogen lone pair orbital and the orbitals in the acceptor group. The orbitals displayed in Figure 7 are rather strongly delocalized π NLMOs of the bridge, the donor, and the acceptor groups. The predominant role of the π-bridge orbital in the enhancement suggests that the enhancement mechanism of γ is related to orbital overlap between the twisted fragments.

The absorption spectra of **TMC-2** obtained with the nonhybrid PBE, hybrid PBE0 and CAM-B3LYP, and intermediate HALFX functionals are presented in Figure 8. There are two major absorption bands in the visible and UV spectral regions. Resonant two-photon absorption at ~900 nm (1800 nm laser wavelength) results in the change of sign of the averaged γ in the nonhybrid case (see Table 2). In contrast, the visible region linear absorption band is centered at 695 nm according to the hybrid CAM-B3LYP calculations, which leads to a two-photon resonance of γ at ~700 nm (1400 nm laser wavelength, see Table 3). The spectra were computed with homogeneous Lorentzian broadening set to 0.2 eV. Note that the experimental absorption spectrum presented in Figure 1 features the visible band centered at somewhat higher energy than computed, 570 nm, and with a half-width at half-maximum of ~0.3 eV. However, these calculations do not account for solvation effects, and, in the case of **TMC-2**, negative solvatochromism, i.e., blue-shifting of the absorption in more polar solvents, is observed experimentally and is in accord with a zwitterionic ground state and a less polar excited state.[11a,b] Unfortunately, **TMC-2** is insufficiently soluble and aggregate-free in less polar solvents to allow spectroscopy. Note also that the relative band intensities observed experimentally do not agree completely with the computed linear absorption bands. The reason for this is inhomogeneous vibrational broadening of the visible band that is not accounted for in our

Table 3. Dispersion of the Two-Photon Transition Moment of Twisted Chromophore TMC-2 Computed with the CAM-B3LYP Functional

wavelength (nm)	S (10^4 au)	σ_2 (GM)
311	627.00	24 175
327	0.07	2
332	7.70	260
352	16.80	505
453	0.08	1
695	4.06	31

calculations. The variance between the values of two-photon absorption cross sections (Tables 1 and 3) can also be explained by this fact along with the well-known underestimation of the excitation energies commonly observed in DFT calculations.[23] It has to be noted, though, that direct comparison of TPA cross-section values is rather uncertain. Along with the line shape and DFT deficiencies, factors such as solvation effects on hyperpolarizabilities of twisted systems and pulse length dependency of TPA cross sections[24] have to be accounted for. Two measured values of two-photon absorption cross sections can, with a certain degree of reliability, be related to the three last rows in Table 3. Indeed, the measured nonresonant TPA cross section value of 1.5 GM at 1170 nm laser wavelength, when extrapolated to the resonant wavelength, can be related to the resonant TPA cross section of 31 GM computed at the lowest excitation of 695 nm. Note again that the experimental measurement was not resonant, although it was performed close to the two-photon resonance according to the UV−vis absorption spectrum in Figure 2. The measured TPA cross section of 8.87 GM at 775 nm laser wavelength can be related to the resonant TPA cross section of 1 GM computed at 453 nm, although the experimental value is clearly off-resonant (see Figure 2). On the other hand, the computed excitation at 453 nm is weak, with a small transition moment (see Figure 8), whereas the next excitation at 352 nm brings about the resonant TPA cross section of 505 GM. The experimentally measured TPA cross section therefore falls between these two calculated values. All in all, comparison between computation and experiment requires additional work and consideration from both the experimental and theoretical sides. Note that experiment is always pulse-, intensity-, and polarization-dependent. Even for the reference compounds, the experimental results vary significantly between different research groups.[25]

CONCLUSIONS

We have shown both experimentally and theoretically that, for a relatively simple twisted π-electron system chromophore, **TMC-2**, n_2 is large and *positive* (1.87×10^{-13} cm^2/W) at 775 nm, relatively close to the one-photon resonance, leading

dx.doi.org/10.1021/ja1113112 |J. Am. Chem. Soc. 2011, 133, 6675–6680

to self-focusing. Furthermore, the **TMC-2** third-order response features a very low two-photon absorption coefficient, corresponding to minimal nonlinear optical losses and a remarkably low T factor, $\alpha_2\lambda/n_2$, of 0.308 at 775 nm. These characteristics are attributed to closely spaced singlet biradical and zwitterionic states and offer promise for applications in all-optical switching. Current efforts are focused on realizing and characterizing chromophores with even more attractive third-order properties.

■ ASSOCIATED CONTENT

Supporting Information. Complete refs19 and 20, and experimental and computational methods. This material is available free of charge via the Internet at http://pubs.acs.org.

■ AUTHOR INFORMATION

Corresponding Authors

marek.samoc@pwr.wroc.pl; a-facchetti@northwestern.edu; agren@theochem.kth.se; t-marks@northwestern.edu; pnprasad@buffalo.edu

■ ACKNOWLEDGMENT

The authors are grateful to Zilvinas Rinkevicius of Royal Institute of Technology, Sweden, and Jochen Autschbach of SUNY at Buffalo for help with calculations. T.J.M. thanks DARPA/ONR (SP01P7001R-A1/N00014-00-C) and the NSF-Europe program (DMR-0353831) for support of this research at Northwestern. M.S. thanks the Foundation for Polish Science Welcome Programme for support. N.W. thanks Toyobo Corp. for a study leave.

■ REFERENCES

(1) Reinhardt, B. A. *Photon. Sci. News* **1999**, *4*, 21.

(2) Prasad, P. N.; Reinhardt, B. A. *Chem. Mater.* **1990**, *2*, 660–669.

(3) He, G. S.; Tan, L. S.; Zheng, Q.; Prasad, P. N. *Chem. Rev.* **2008**, *108*, 1245–1330.

(4) (a) Isborn, C. M.; Leclercq, A.; Vila, F. D.; Dalton, L. R.; Brédas, J. L.; Eichinger, B. E.; Robinson, B. H. *J. Phys. Chem. A* **2007**, *111*, 1319–1327. (b) Marder, S. R.; Beratan, D. N.; Cheng, L.-T. *Science* **1991**, *252*, 103–106. (c) Oudar, J. L.; Chemla, D. S. *J. Chem. Phys.* **1977**, *66*, 2664–2668.

(5) (a) Abbotto, A.; Beverina, L.; Bradamante, S.; Facchetti, A.; Klein, C.; Pagani, G. A.; Redi-Abshiro, M.; Wortmann, R. *Chem.—Eur. J.* **2003**, *9*, 1991–2007. (b) Coe, B. J.; Jones, L. A.; Harris, J. A.; Brunschwig, B. S.; Asselberghs, I.; Clays, K.; Persoons, A.; Garin, J.; Orduna, J. *J. Am. Chem. Soc.* **2004**, *126*, 3880–3891. (c) Datta, A.; Pati, S. K. *Chem.—Eur. J.* **2005**, *11*, 4961–4969. (d) Liao, Y.; Bhattacharjee, S.; Firestone, K. A.; Eichinger, B. E.; Paranji, R.; Anderson, C. A.; Robinson, B. H.; Reid, P. J.; Dalton, L. R. *J. Am. Chem. Soc.* **2006**, *128*, 6847–6853. (e) Marder, S. R.; Kippelen, B.; Jen, A. K. Y.; Peyghambarian, N. *Nature* **1997**, *388*, 845–851.

(6) (a) Albert, I. D. L.; Marks, T. J.; Ratner, M. A. *J. Am. Chem. Soc.* **1997**, *119*, 3155–3156. (b) Albert, I. D. L.; Marks, T. J.; Ratner, M. A. *Chem. Mater.* **1998**, *10*, 753–762. (c) Varanasi, P. R.; Jen, A. K. Y.; Chandrasekhar, J.; Namboothiri, I. N. N.; Rathna, A. *J. Am. Chem. Soc.* **1996**, *118*, 12443–12448.

(7) Galvan-Gonzalez, A.; Belfield, K. D.; Stegeman, G. I.; Canva, M.; Marder, S. R.; Staub, K.; Levina, G.; Twieg, R. J. *J. Appl. Phys.* **2003**, *94*, 756–763.

(8) (a) Kang, H.; Zhu, P.; Yang, Y.; Facchetti, A.; Marks, T. J. *J. Am. Chem. Soc.* **2004**, *126*, 15974–15975. (b) Ostroverkhov, V.; Petschek, R. G.; Singer, K. D.; Twieg, R. J. *Chem. Phys. Lett.* **2001**, *340*, 109–115. (c) Traber, B.; Wolff, J. J.; Rominger, F.; Oeser, T.; Gleiter, R.; Goebel, M.; Wortmann, R. *Chem.—Eur. J.* **2004**, *10*, 1227–1238. (d) Wolff, J. J.; Siegler, F.; Matschiner, R.; Wortmann, R. *Angew. Chem. Int. Ed.* **2000**, *39*, 1436. (e) Wortmann, R.; Lebus-Henn, S.; Reis, H.; Papadopoulos, M. G. *J. Mol. Struct.: THEOCHEM* **2003**, *633*, 217–226. (f) Yang, M.; Champagne, B. *J. Phys. Chem. A* **2003**, *107*, 3942–3951.

(9) (a) Kuzyk, M. G. *Phys. Rev. Lett.* **2000**, *85*, 1218. (b) Tripathy, K.; Moreno, J. P.; Kuzyk, M. G.; Coe, B. J.; Clays, K.; Kelley, A. M. *J. Chem. Phys.* **2004**, *121*, 7932–7945.

(10) (a) Albert, I. D. L.; Marks, T. J.; Ratner, M. A. *J. Am. Chem. Soc.* **1997**, *119*, 6575–6582. (b) Keinan, S.; Zojer, E.; Brédas, J.-L.; Ratner, M. A.; Marks, T. J. *J. Mol. Struct.: THEOCHEM* **2003**, *633*, 227–235.

(11) (a) Wang, Y.; Frattarelli, D. L.; Facchetti, A.; Cariati, E.; Righetto, S.; Ugo, R.; Zuccaccia, C.; Macchioni, A.; Stern, C. L.; Ratner, M. A.; Marks, T. J. *J. Phys. Chem. C* **2008**, *112*, 8005–8015. (b) Kang, H.; Facchetti, A.; Jiang, H.; Cariati, E.; Righetto, S.; Ugo, R.; Zuccaccia, C.; Macchioni, A.; Stern, C. L.; Liu, Z. F.; Ho, S. T.; Brown, E. C.; Ratner, M. A.; Marks, T. J. *J. Am. Chem. Soc.* **2007**, *129*, 3267–3286. (c) Kang, H.; Facchetti, A.; Stern, C. L.; Rheingold, A. L.; Kassel, W. S.; Marks, T. J. *Org. Lett.* **2005**, *7*, 3721–3724. (d) Kang, H.; Facchetti, A.; Zhu, P. W.; Jiang, H.; Yang, Y.; Cariati, E.; Righetto, S.; Ugo, R.; Zuccaccia, C.; Macchioni, A.; Stern, C. L.; Liu, Z. F.; Ho, S. T.; Marks, T. J. *Angew. Chem. Int. Ed.* **2005**, *44*, 7922–7925.

(12) (a) Brown, E. C.; Marks, T. J.; Ratner, M. A. *J. Phys. Chem. B* **2007**, *112*, 44–50. (b) Isborn, C. M.; Davidson, E. R.; Robinson, B. H. *J. Phys. Chem. A* **2006**, *110*, 7189–7196.

(13) (a) Nakano, M.; Minami, T.; Fukui, H.; Yoneda, K.; Shigeta, Y.; Kishi, R.; Champagne, B.; Botek, E. *Chem. Phys. Lett.* **2010**, *501*, 140. (b) Nakano, M.; Champagne, B.; Botek, E.; Ohta, K.; Kamada, K.; Kubo, T. *J. Chem. Phys.* **2010**, *133*, 154302.

(14) (a) Sheik-Bahae, M.; Said, A. A.; Van Stryland, E. W. *Opt. Lett.* **1989**, *14*, 955–957. (b) Sheik-Bahae, M.; Said, A. A.; Wei, T. H.; Hagan, D. J.; Van Stryland, E. W. *IEEE J. Quantum Elect.* **1990**, *26*, 760–769. (c) Van Stryland, E. W.; Sheik-Bahae, M. *Opt. Eng.* **1998**, *60*, 655.

(15) Samoc, M.; Samoc, A.; Humphrey, M. G.; Cifuentes, M. P.; Luther-Davies, B.; Fleitz, P. A. *Mol. Cryst. Liq. Cryst.* **2008**, *485*, 146/[894]–154/[902].

(16) Lee, K.-S.; Samoc, M.; Hwang, D. H.; Zyung, T. H. In *Advanced functional molecules and polymers*, Vol. 3; Nalwa, H., Ed.; Gordon and Breach: The Netherlands, 2001.

(17) Hales, J. M.; Matichak, J.; Barlow, S.; Ohira, S.; Yesudas, K.; Bredas, J.-L.; Perry, J. W.; Marder, S. R. *Science* **2010**, *327*, 1485–1488.

(18) Samoc, A.; Samoc, M.; Woodruff, M.; Luther-Davies, B. *Opt. Lett.* **1995**, *20*, 1241–1243.

(19) Baerends, E. J.; et al. *Amsterdam Density Functional, SCM*; Theoretical Chemistry, Vrije Universiteit: Amsterdam, The Netherlands.

(20) Angeli, C.; et al. *Dalton, A molecular electronic structure program*, Release 2.0; 2005.

(21) Ye, A.; Patchkovskii, S.; Autschbach, J. *J. Chem. Phys.* **2007**, *127*, 074104.

(22) Weinhold, F. In *Encyclopedia of computational chemistry*; von Ragué Schleyer, P., Ed.; John Wiley & Sons: Chichester, 1998; pp 1792−1811.

(23) (a) Baev, A.; Prasad, P. N.; Samoc, M. *J. Chem. Phys.* **2005**, *122*, 224309. (b) Salek, P.; Ågren, H.; Baev, A.; Prasad, P. N. *J. Phys. Chem. A* **2005**, *109*, 11037–11042.

(24) Gel'mukhanov, F.; Baev, A.; Macak, P.; Luo, Y.; Ågren, H. *J. Opt. Soc. Am. B* **2002**, *19*, 937–945.

(25) Jhat, P. C.; Wang; Y.; Luo, Y.; Agren, H. *Metamaterials 2006, International Symposium on Biophotonics, Nanophotonics, and Metamaterials*; 2006.